

Microscopic View on Short-Range Wetting at the Free Surface of the Binary Metallic Liquid Gallium-Bismuth: An X-ray Reflectivity and Square Gradient Theory Study.

Patrick Huber,* Oleg Shpyrko, and Peter Pershan

Department of Physics, Harvard University, Cambridge MA 02138 (U. S. A.)

Ben Ocko and Elaine DiMasi

Department of Physics, Brookhaven National Lab, Upton NY 11973 (U. S. A.)

Moshe Deutsch

Department of Physics, Bar-Ilan University, Ramat-Gan 52900 (Israel)

(Dated: May 1, 2019)

We present an x-ray reflectivity study of wetting at the free surface of the binary liquid metal gallium-bismuth (Ga-Bi) in the region where the bulk phase separates into Bi-rich and Ga-rich liquid phases. The measurements reveal the evolution of the microscopic structure of wetting films of the Bi-rich, low-surface-tension phase along different paths in the bulk phase diagram. A balance between the surface potential preferring the Bi-rich phase and the gravitational potential which favors the Ga-rich phase at the surface pins the interface of the two demixed liquid metallic phases close to the free surface. This enables us to resolve it on an Ångström level and to apply a mean-field, square gradient model extended by thermally activated capillary waves as dominant thermal fluctuations. The sole free parameter of the gradient model, i.e. the so-called influence parameter, κ , is determined from our measurements. Relying on a calculation of the liquid/liquid interfacial tension that makes it possible to distinguish between intrinsic and capillary wave contributions to the interfacial structure we estimate that fluctuations affect the observed short-range, *complete* wetting phenomena only marginally. A *critical* wetting transition that should be sensitive to thermal fluctuations seems to be absent in this binary metallic alloy.

PACS numbers: 61.25.Mv, 61.30.Hn, 68.10.-m, 61.10.-i

I. INTRODUCTION

The concept of a wetting transition that was introduced independently by Cahn¹ and Ebner and Saam² in 1977, has stimulated a substantial amount of theoretical and experimental work^{3,4,5,6,7}. Due to its critical character it is not only important for a huge variety of technological processes ranging from alloying to the flow of liquids, but has the character of an extraordinarily versatile and universal physical concept, which can be used to probe fundamental predictions of statistical physics. For example, as shall be depicted in more detail later on, it can be employed in the case of wetting dominated by short-range interactions (SRW) in order to test the predictions for the break-down of mean-field behavior and the necessary "transition" to a renormalization group regime, where this surface phenomenon is significantly affected by thermal fluctuations.

A wetting transition occurs for two fluid phases in or near equilibrium in contact with a third inert phase, e.g., the container wall or the liquid-vapor interface. On approaching the coexistence critical point the fluid phase that is energetically favored at the interface forms a wetting film that intrudes between the inert phase and the other fluid phase. In general, this surface phenomenon is a delicate function of both the macroscopic thermodynamics of the bulk phases and the microscopic interactions.

Whereas one of the seminal theoretical works² on the wetting transition gave a microscopic view on this phenomenon, experimental results at this same level of detail were only recently obtained through application of X-ray and neutron reflection and diffraction techniques^{8,9,10}. Moreover, almost all of these experimental studies dealt with systems, like methanol-cyclohexane and other organic materials, that are dominated by long-range van-der-Waals interactions⁷. The principal exceptions to this are the studies of the binary metallic systems gallium-lead (Ga-Pb)¹¹, gallium-thallium (Ga-Tl)¹², and gallium-bismuth (Ga-Bi)¹³, for which the dominant interactions are short-range.

Here, we will present an x-ray reflectivity study of wetting phenomena that occur at the free surface in the binary metallic liquid Ga-Bi when the bulk demixes in two liquid phases, i.e. a Bi-rich and a Ga-rich liquid phase. The fact that the wetting geometry pins the liquid/liquid (1/1) interface that divides the two liquids to the surface allows measurements that show the compositional profile of the wetting film at the Ångström level. We will show results for the structure of the film as it evolves towards the gravity-thinned film. Through a combination of this structural information and the bulk thermodynamics of the system, it was possible to extract detailed information on the dominant interaction parameters governing the surface phenomenology. We will show that a square gradient theory that is combined with the effects

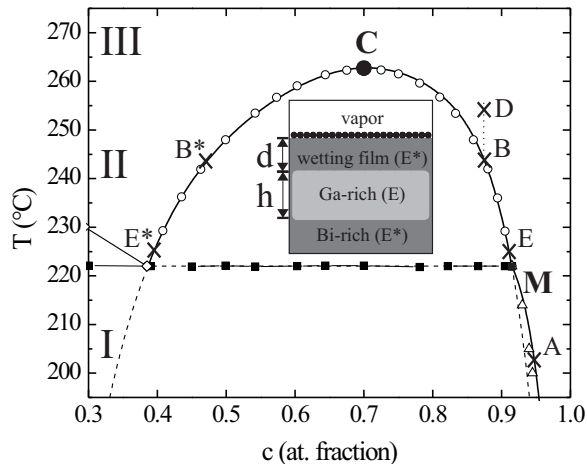


FIG. 1: The atomic fraction (c)-temperature(T) bulk phase diagram of Ga-Bi. The symbols indicate coexistence lines of Predel's phase diagram¹⁴. The lines show the phase boundaries calculated from thermodynamic data¹⁵. The dashed lines represent the metastable extension of the (l/l) coexistence line below T_M . The points are: C-bulk critical point, M-monotectic point, A,B,D,E-points on the experimental path. The insets illustrate the surface and bulk phases. In region II the wetting film is 50 Å thick and the Ga-rich fluid is 5 mm thick. The bold circled in the insets symbolize the Bi-monolayer.

of thermally excited capillary waves provides a reasonable description of that interface. In fact, we will be able to extract the sole free parameter of that model, i.e. the influence parameter κ . This, in turn, will allow us to distinguish between intrinsic (mean-field) and fluctuation (capillary waves) contributions to the interfacial structure. On the basis of this distinction we will estimate the influence of fluctuations on the observed SRW at the free surface.

The paper is structured as follows: In the first section, we introduce the bulk phase diagram of Ga-Bi and relate its topology to the wetting transitions observable at the free surface of this binary alloy. X-ray reflectivity measurements on the wetting films along different paths in the bulk phase diagram will be discussed in the second section. The third section will focus on the thermodynamics and structure of the liquid-liquid interface. In this section we will develop a square gradient theory in order to model the concentration profile at the liquid/liquid interface. Finally, in the last section we will provide a more general discussion of the rich wetting phenomenology at the free surface of this binary liquid metal.

II. BULK & SURFACE THERMODYNAMICS

The bulk phase diagram of Ga-Bi, cp. Fig. 1, was measured by Predel with differential thermal analysis¹⁴. It is dominated by a miscibility gap with consolute point C (critical temperature $T_C = 262.8^\circ\text{C}$, critical atomic fraction of Ga, $c_{\text{crit}} = 0.7$) and a monotectic temperature, $T_M = 222^\circ\text{C}$. In the part of region I with $T < T_M$, solid Bi coexists with a Ga-rich liquid. At T_M , the boundary takes place in the bulk due to the liquidisation of pure Bi. For $T_M < T < T_C$ (region II), the bulk separates into two immiscible phases, a high density Bi-rich liquid and a low density Ga-rich liquid. The heavier Bi-rich phase is macroscopically separated from the lighter Ga-rich phase due to gravity. In region III, beyond the miscibility gap, a homogeneous liquid is found.

Following the observation of Perepezko¹⁶ that on cooling fine Ga-rich droplets are coated by a Bi-rich solid phase, Nattland et. al. studied the liquid-vapor interface in region II using ellipsometry. They found that a thin Bi-rich film intrudes between the vapor and the Ga-rich subphase in defiance of gravity¹³, as implied by the illustration in Fig. 1. This was a clear example of the critical point wetting in binary systems that was described by Cahn¹. On approaching to point C, the Bi-rich phase necessarily becomes energetically favored at the free surface and as a result it forms the wetting film that intrudes between the Ga-rich subphase and the surface. In fact the situation is slightly more complicated since x-ray studies indicate that throughout region III the free surface is coated by a monolayer of pure Bi¹⁷. More recently we showed that on heating the binary liquid a thicker wetting layer of Bi rich liquid forms between the Bi monolayer and the bulk Ga rich liquid. This appears to be an unusual example of complete wetting that is pinned to the monotectic temperature T_M . This phenomenon was first discussed by Dietrich and Schick in order to explain an analogous finding in the binary metallic alloy Ga-Pb^{11,18}. The nature of this apparent coincidence of a surface transition with the first order transition in the bulk at T_M can most easily be illustrated by a transformation of the (c, T)-diagram to the appropriate chemical potential-temperature (μ, T)-diagram that is depicted in Fig. 2(a) for Ga-Bi. The axis are temperature, T , the difference ($\mu_{\text{Bi}} - \mu_{\text{Ga}}$) of the chemical potentials of the single species, and their sum ($\mu_{\text{Bi}} + \mu_{\text{Ga}}$). In this plot, the (l/l)-miscibility gap of Fig. 1, which strictly spoken is a liquid/liquid/vapor (l/l/v) coexistence boundary, transforms into a (l/l/v)-triple line extending from M to C (solid circles). At M this triple line intersects with another triple line, i.e. the solid/liquid/vapor (s/l/v)-coexistence line (solid squares), rendering M a *tetra point* of four phase coexistence⁷⁰. At M a solid Bi, a Ga-rich, a Ga-poor phase, and the vapor coexist.

The thermodynamics by which the surface transition at M is pinned by the bulk phase transition is obvious if one considers the topology of the (μ, T)-plot in the prox-

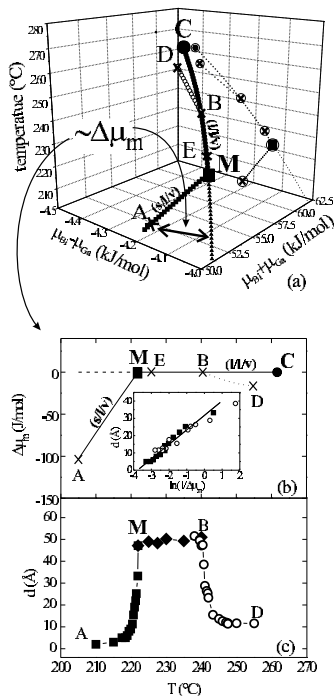


FIG. 2: (a) The chemical potential (μ)-temperature (T) bulk phase diagram of Ga-Bi. The axes are temperature, T , the difference ($\mu_{\text{Bi}} - \mu_{\text{Ga}}$) of the chemical potentials of the single species, and their sum ($\mu_{\text{Bi}} + \mu_{\text{Ga}}$). The solid symbols indicate the following coexistence lines: (solid circles) liquid/liquid/vapor (l/l/v) triple line, (solid squares) solid/liquid/vapor (s/l/v) triple line, (small triangles) metastable extension of the liquid/liquid/vapor (l/l/v) triple line below T_M , (open circles) experimental path B-D probing complete wetting. The points are: C-bulk critical point, M-monotectic point, A,B,D,E-points on the experimental path. To illustrate the 3-dimensional structure of the phase diagram, a projection of the phase boundary lines on the $(\mu_{\text{Bi}} - \mu_{\text{Ga}}, T)$ plane is drawn in the plot. The symbols surrounded by a circle show where the aforementioned characteristic points fall on this projection. (b) $(\Delta\mu_m, T)$ phase diagram: (A-M) is the (s/l/v), and (M-C) is the (l/l/v) coexistence line. The path B-D is in the single phase region, and M and C are the monotectic and critical points. Inset: effective wetting layer thickness d on A \rightarrow M (squares) and B \rightarrow D (open circles). The solid line is a fit to the A \rightarrow M d -values. (c) The measured d along the experimental path.

imity of M. The wetting of the free surface by the Bi-rich phase as well as the bulk transition are driven by the excess free energy, $\Delta\mu_m$, of the Bi-rich phase over that of the Ga-rich liquid phase⁵. This quantity is proportional to the distance between the (l/l/v)-triple line and any other line leading off (l/l/v)-coexistence, e.g. the (s/l/v)-triple line (A \rightarrow M) or the line B \rightarrow D in Fig. 2(a). The wetting thermodynamics is displayed in a slightly simpler way by the plot $\Delta\mu_m$ vs. T in Fig. 2(b). In this figure for $T > T_M$, the (l/l/v) coexistence line transforms into a horizontal straight line that extends from M to C. For $T < T_M$ the horizontal dashed line indicates the

metastable (l/l/v) extension of the coexistence and that is above the solid-Bi/Ga-rich/vapor (s/l/v) coexistence line that goes from M to A. This illustrates the observation by Dietrich and Schick¹⁸ that the path A \rightarrow M leads to coexistence, and thus complete wetting is dictated by the topology of the phase diagram.

A more quantitative understanding of the surface wetting phenomena can be developed by analyzing the grand canonical potential, Ω_S per unit area A of the surface⁵: $\Omega_S/A = d\Delta\mu + \gamma_0 e^{-d/\xi}$. Here, d is the wetting film thickness, ξ is the decay length of a short-range, exponential decaying potential, γ_0 its amplitude and A an arbitrary surface area. The quantity $\Delta\mu$ comprises all energies that are responsible for a shift off true bulk (l/l/v) coexistence, i.e. the aforementioned quantity $\Delta\mu_m$. The formation of the heavier Bi-rich wetting layer at some height, h , above its bulk reservoir costs an extra gravitational energy $\Delta\mu_g = g\Delta\rho_m h$ where $\Delta\rho_m$ is the mass density difference between the two phases. Minimization of Ω_S in respect to d then yields the equilibrium wetting film thickness of the Bi-rich phase $d = \xi \ln(\gamma_0/\Delta\mu)$. In fact the gravitational energy is only significant in comparison with the other terms for very small values $\Delta\mu_m$ and for most of the data shown in Fig. 2 the gravitational term can be neglected, allowing of $\Delta\mu = \Delta\mu_m$. Thus, one expects a logarithmic increase of the wetting film thickness upon approaching M from A that is given by $d = \xi \ln(\gamma_0/\Delta\mu_m)$, in agreement with the experimental finding that was presented in our recent Physical Review Letter on this phenomenon - cp. inset in Fig. 2(b)¹⁹. The slight deviations for small values of $\Delta\mu_m$, as well as the finite value of $d \sim 50\text{\AA}$ along the coexistence line M \rightarrow B are due to the gravitational term. Since this approach of the (l/l/v)-coexistence line ends in M with its four phase coexistence, the phenomenon is properly described as *tetra point wetting*. As demonstrated here, the occurrence of this complete wetting phenomenon at the surface is an intrinsic feature of the bulk phase diagram.

In this paper we shall present additional x-ray reflectivity measurements that show the evolution of the wetting film on approaching coexistence from point D in regime III, and hence along a path probing complete wetting that is not dictated by the topology intrinsic to the bulk phase diagram, but rather by the experimenter's choice of the overall atomic fraction of Ga in the sample c_{nom} , i.e. the path B \rightarrow D in Fig. 1 and Fig. 2(a,b). Furthermore, we will probe the wetting film structure along an on-(l/l/v) coexistence path B \rightarrow E.

III. X-RAY REFLECTIVITY MEASUREMENTS

A. Experiment

1. Sample Preparation & Sample Environment

The Ga-Bi alloy was prepared in an inert-gas box using $> 99.9999\%$ pure metals. A solid Bi pellet was covered

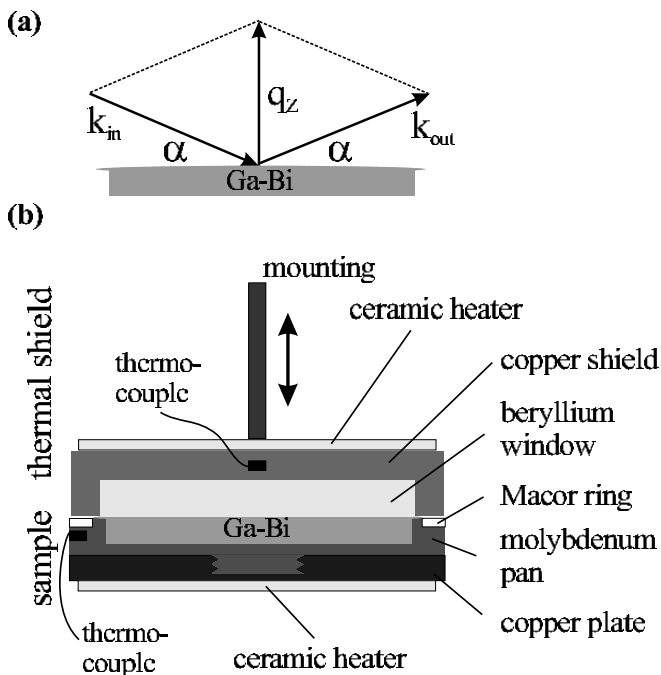


FIG. 3: (a) scattering geometry (b) Sketch of the experimental setup. The arrow close to the mounting indicates the variable position of the thermal shield in respect to the sample surface.

by an amount of liquid Ga required for a nominal concentration $c_{nom} = 88$ at% Ga. It was then transferred in air into an ultrahigh vacuum chamber. A 24-hour period of bake-out yielded a pressure of 10^{-10} torr. The residual surface oxide on the liquid's surface was removed by sputtering with Ar^+ ions. Using thermocouple sensors and an active temperature control on both sample pan and its adjacent thermal shield a temperature stability and uniformity of $\pm 0.05^\circ C$ was achieved. A sketch of the experimental setup, sample environment resp. can be found in Fig. 3(b).

A challenge in all x-ray reflectivity measurements of liquid metals is the high surface tension of these systems, e.g. pure Ga has a surface tension of ≈ 700 mN/m. It often prevents liquid metal from wetting non-reactive container walls or substrates. This also leads to large curvatures of the liquid surface hampering x-ray reflectivity measurements²⁰. Remnant oxide layers that exists at the liquid/container, liquid/substrate interface resp. even enhance this non-wetting effect; therefore, we removed these oxide layers from the Mo sample pan by sputtering with Ar^+ ions, at a sputter current of 25 mA and a sputter voltage of 2 kV, and could reach wetting of the Mo crucible by the liquid metal. This resulted in small curvatures of the free surface as was judged by eye and later on by x-ray reflectivity measurements. The resulting flat surfaces facilitated the accumulation of reliable x-ray reflectivity data sets, particularly for small incident angles, α . On the other hand, the wetting of the container wall by the liquid alloy promoted some spilling

of the liquid during the sample movements that were necessary to track the sample position during the reflectivity scan. We circumvented this problem by installing a ceramic ring that surrounded the sample pan. The ceramics is not wetted by the liquid metal and, therefore, inhibits any liquid flow at the outermost circumference of the sample pan.

Another experimental challenge is related to x-ray reflectivity measurements from liquids in general. The surface of a liquid is sensitive to any kind of vibrations or acoustic noise. In order to obtain a stable reflected signal from the liquid surface, we mounted our UHV chamber on an active vibration isolation²⁰.

2. X-Ray Reflectivity

X-ray reflectivity measurements were carried out using the liquid surface reflectometer at beamline X22B at National Synchrotron Light Source with an x-ray wavelength $\lambda = 1.54 \text{ \AA}$. Background and bulk scattering were subtracted from the specular signal by displacing the detector out of the reflection plane by 0.3° . The scattering geometry can be found as inset in Fig. 3. The intensity $R(q_z)$, reflected from the surface, is measured as a function of the normal component $q_z = 4\pi/\lambda \sin(\alpha)$ of the momentum transfer and yields information on the surface-normal structure of the electron density $\rho(z)$ as described by the so-called master formula²¹. This formula relates the Fourier-transformed electron density gradient with the experimentally obtained R/R_F . The symbol R_F denotes the Fresnel reflectivity that is expected from an ideally flat and sharp surface having the electron density of the Ga-rich liquid. The standard procedure for determining the electron density profile $\rho(z)$ from the measured reflectivity $R(q_z)$ is to construct a simple and physically meaningful density model and to fit its Fourier transform to experimentally obtained data sets of R/R_F ²². We employ a three-box model⁹, where the upper box represents the Gibbs-adsorbed Bi monolayer the second represents the Bi-rich wetting film and the lower box represents the bulk liquid. The relative electron densities of these boxes correspond to pure Bi (top box) and to the electron density of the Bi-rich wetting film, ρ . The quantity ρ_{sub} denotes the electron density of the Ga-rich subphase. In the simplest approximation the electron density profiles of the interfaces between the different phases can be described analytically by error-functions. The relevant model for this problem includes three error-functions (erf)-diffusenesses for the following interfaces: vapor/Bi monolayer, Bi monolayer/Bi rich film, Bi rich film/Ga rich bulk phase. The first two interfaces describing the monolayer feature were remained unchanged in the presence of the Bi-rich film, while only the diffuseness of the Bi rich film/Ga rich bulk phase interface, σ_{obs} , was a variable parameter as a function of T . The model also included size parameters that describe the thickness of the two upper boxes. The box that de-

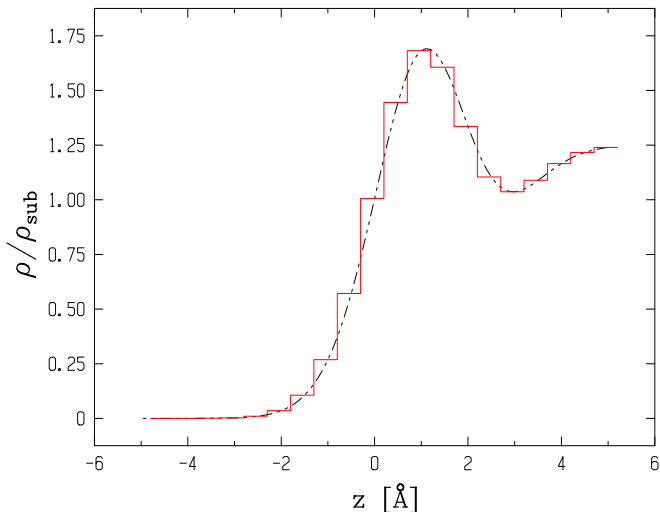


FIG. 4: Illustration of the approximation of the analytic electron density profile (dashed line) by thin slabs in order to apply the Parratt formalism. Here, only the region close to the monolayer feature is depicted.

scribes the bulk sub-phase extends to infinity. During the fitting the thickness of the monolayer box was kept constant while the thickness of the Bi-rich film was allowed to vary.

The use of the master formula tacitly assumes the validity of the Born approximation. This assumption holds true for wave vectors, q_z , much larger than the value of the critical wavevector q_c of the Ga-rich subphase, where multi-scattering effects can be neglected²³. Here, however, we will be interested in features corresponding to 30-60 Å thick wetting films, which when translated to momentum-space corresponds to features in q_z around 0.05-0.1 Å⁻¹ that are comparable to the value of the critical wavevector $q_c \approx 0.05 \text{ Å}^{-1}$ (The q_c -values change only slightly depending on T , cp. Table I). In order to deal with this we resort to the recursive Parratt formalism²⁴ for q_z -values close to q_c . In this formalism one develops a 2x2 matrix that relates the amplitudes and phases for the incoming and outgoing waves on both sides of a slab of arbitrary dielectric constant. For the present problem we approximate the above mentioned three-box profile by a large number of thinner slabs whose amplitudes are chosen to follow the envelope of the analytic profile - cp. fig. 4. Typically the number of slabs was of the order of 300.

B. Wetting film structures approaching (1/1/v)-coexistence

Here we will present x-ray reflectivity measurements from the free surface of Ga-Bi along a path approaching (1/1/v) coexistence from the homogeneous part of the bulk phase diagram (regime III), i.e. the path D→B. This path, particularly the position of its characteristic

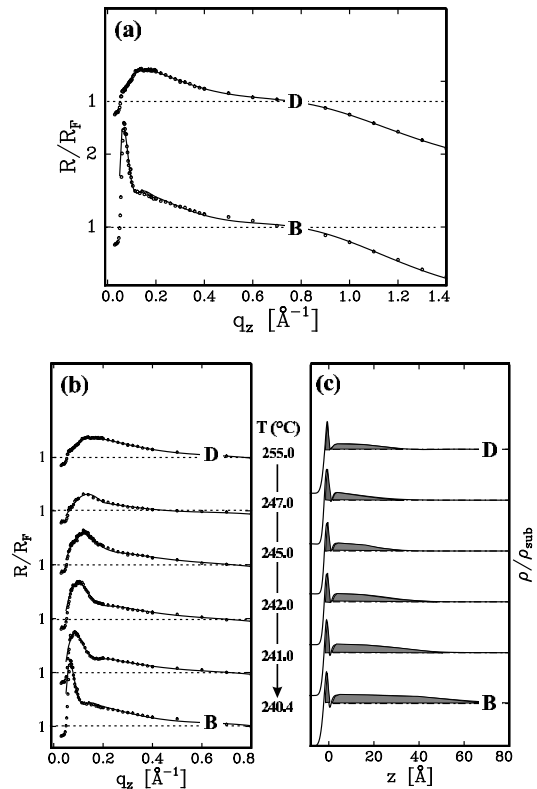


FIG. 5: (a) Normalized reflectivities R/R_F for selected points D and B corresponding to $T_D=255.0^\circ\text{C}$, $T_B = 240.4^\circ\text{C}$. Dashed lines indicate $R/R_F = 1$. (b) T -dependent normalized reflectivities R/R_F while approaching coexistence on path D → B along with fits. Dashed lines indicate $R/R_F = 1$. (c) Electron density profiles ρ/ρ_{sub} . All regions with $\rho/\rho_{\text{sub}} > 1$ indicating Bi-enrichment as compared with the Ga-rich subphase are gray shaded.

point B, is solely determined by the overall atomic fraction of Ga in the sample pan, c_{nom} . While cooling this path intersects the (1/1/v) triple line (cp. Fig. 2) at the point B, corresponding to temperature T_B of the miscibility boundary (cp. Fig. 1). For $T < T_B$ the heretofore homogeneous bulk liquid phase separates into the heavier Bi rich liquid that settles towards the bottom of the pan and the lighter Ga rich liquid on top. The actual position in the (c,T) -plane was chosen from consideration of the vanishing electron density contrast between Ga-rich and Bi-rich phase upon approaching C on the one hand or the (1/1/v) triple line (cp. Fig. 2(a)) enforcing the spinodal demixing of the afore homogeneous bulk liquid. In our case, its position in the (c,T) -plane was chosen after a consideration of the vanishing electron density contrast between Ga-rich and Bi-rich phase upon approaching C, on the one hand, and a reasonably "long path" on (1/1/v) coexistence on the other hand. The compromise was a value of about 12% for c_{nom} , which corresponds to $T_B = 240.4^\circ\text{C}$.

X-ray reflectivity $R(q_z)$ was measured at selected temperatures on path D→B. In order to avoid artifacts as-

sociated with the fact that the evolution of the wetting film is governed by slow diffusion processes^{25,26,27} equilibration was monitored by continuous taking repeated reflectivity scans following increments of small temperature steps of 0.5°C . Typically the measured reflectivity fluctuated wildly for a couple of hours, after which it slowly evolved to a stable equilibrium. The fits (lines) to these "equilibrium" R/R_F (points) are shown in Fig. 5(a,b), and the corresponding $\rho(z)$ profiles - in Fig. 5(c). At point D [$T_D = 255^\circ\text{C}$], typical of region III, R/R_F exhibits a broad peak at low q_z as well as an increased intensity around $q_z = 0.8\text{\AA}^{-1}$. The corresponding electron density profile $\rho(z)$ obtained from the fit indicates a thin, inhomogeneous film of increased electron density (as compared with ρ_{sub}) close to the surface along with a peak right at the surface. It is consistent with a segregated monolayer of pure Bi along with a thin layer of a Bi-enriched phase. As the temperature is decreased towards B, the peak is gradually shifting to lower q_z and its width decreases. This behavior manifests the continuous growth in thickness of the wetting layer upon approaching T_B and is in agreement with the thermodynamic path probing complete wetting: $\Delta\mu_m \rightarrow 0$ on path D \rightarrow B.

Our experimental data clearly indicate film structures dominated by sizeable gradients in the electron density, which contrasts with frequently used "homogeneous slab" models, but is in agreement with theoretical calculations. These range from density functional calculations via square gradient approximations to Monte Carlo simulations for wetting transitions at hard walls^{2,28,29}. Inhomogeneous profiles have also been observed experimentally in microscopically resolved wetting transitions for systems dominated by long-range van-der-Waals interactions^{8,30}. Clearly detailed interpretation of the inhomogeneity for the GaBi wetting films will require either a density functional analysis, or some other equivalent approach. Nevertheless, even a simple model approximating the wetting layer by a slab of thickness d allows a reliable determination of the surface potential governing this complete wetting transition. In order to do so, effective film thicknesses d have been extracted from the $\rho(z)$ profiles. In Fig. 2(c) we show plots of these d -values versus both T and $\Delta\mu_m$. The last plot shows the expected logarithmic behavior and allows determination of the values for the parameters of the short-range potential, i.e. $\gamma_0 = 400\text{mN/m}$ and $\xi = 5.4\text{\AA}$ ¹⁹. Moreover, agreement between the new (d, μ_m) -behavior along $D \rightarrow B$ and the data for the path $A \rightarrow M$ provides an experimental prove that both paths have the same thermodynamic character, i.e. they probe complete wetting: $\Delta\mu_m \rightarrow 0$ on path $A \rightarrow M$ and $D \rightarrow B$.

C. Wetting film structures: On (1/1/v)-coexistence

As discussed before, on cooling from the one phase region (III) we reach the (1/1/v)-coexistence at B. The data for the measured dependence of R/R_F on q_z along

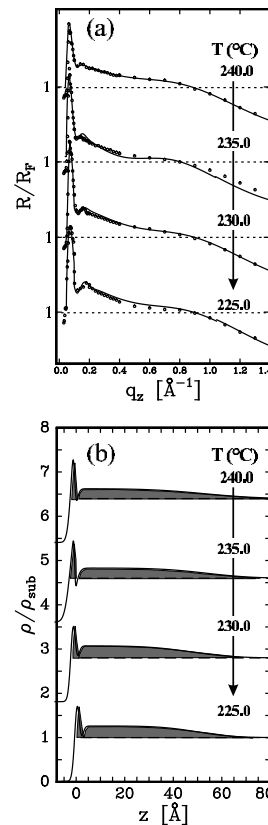


FIG. 6: (a) T-dependent normalized reflectivities R/R_F while leaving coexistence on path $B \rightarrow D$ along with fits. Dashed lines indicate $R/R_F = 1$. With increasing T , each R/R_F is shifted by 1.2. (b) Electron density profiles ρ/ρ_{sub} . All regions with $\rho/\rho_{\text{sub}} > 1$ indicating Bi-enrichment as compared with the Ga-rich subphase are gray shaded.

coexistence between points B and M are shown in Fig. 6(a). The existence of two peaks at low q_z indicates the presence of a fully formed thick film ($\sim 50\text{\AA}$). The solid lines indicate the best fit results corresponding to the real space profiles that are shown in Fig. 6(b). The best fit value for maximum density of the thick film $\rho/\rho_{\text{sub}} = 1.20$ agrees reasonably well with the value of 1.21 that is calculated from the phase diagram at point B.

These results are also reasonably consistent with what is expected for a gravity limited slab of uniform density. Using $\xi = 5.4\text{\AA}$, $\sigma_0 = 400\text{mN/M}$ and the known material constants that make up μ_m (see table I below) the calculated value for $d = d_g = \xi \ln(\sigma_0/\Delta\mu_g) = 15.6\xi = 85\text{\AA}$. In view of the fact that this estimate does not take into account the excess energy associated with associated with concentration gradients across the interfaces some over-estimation of d_g is not too surprising. Nevertheless, this rough calculation does show that the wetting film thickness is expected to be on a mesoscopic rather than on the macroscopic length scale that has been observed for similar wetting geometries in systems governed by long-range, dispersion forces⁶.

Upon cooling from point B to M, the intensity of the

first peak of R/R_F increases as expected due to the gradual increase of the electron density contrast ρ/ρ_{sub} that follows from the increase in the Bi concentration of the bulk phase. Similarly, there is a small shift in the position of the peak indicating that the thickness varies slightly from 53\AA near B to 50\AA near E that follows from the T -dependence of the density contrast $\Delta\rho_m(T)$ as estimated from the bulk phase $\Delta\rho_m(T)$ - cp. Table I. The on-coexistence path B \rightarrow E is too far away from C to expect more pronounced effects on the wetting layer thickness due to a vanishing density contrast or the increase of the influence of the criticality on the interaction potentials^{5,7,31}.

Moreover the gravitational thinning of the on-coexistence wetting film thickness to a length scale comparable to the range of the exponentially decaying short-range interactions prevents testing the influence of long-range, van-der-Waals like atomic interactions on the wetting behavior that is present regardless of whether the system is insulating or metallic^{32,33}.

Finally, we would like to highlight the unique wetting geometry encountered here: The subtle balance between the surface potential that favors the Bi-rich liquid phase at the surface and the gravitational potential that favors the Ga-rich liquid phase above the denser Bi-rich phase, pins the (1/1) interface between the two coexisting phases close to the free surface. It is this property that makes it possible to study the structure of these wetting films. For example, the width of the interface between that film and bulk, σ_{obs} , is the case of the decay of the Kiessig fringes at low q_z . This will be discussed further in the following section.

IV. LIQUID/LIQUID INTERFACE

In this section, we will discuss the microscopic structure of the (1/1)-interface separating the gravitationally thinned film of the Bi-rich phase from the Ga-rich sub-phase along the on-coexistence path B \rightarrow E. We shall first describe a simple square gradient theory for this interface and then extend it by the consideration of thermally excited capillary waves. We will use this theory in order to extract the (1/1)-interfacial profile and the (1/1)-interfacial tension from our measurements of the average surface structure.

A. Square Gradient Theory

At the (1/1)-interface between the two phases, the concentration varies continuously from the bulk concentration of the homogeneous Bi-rich phase, c^I , to the bulk concentration of the homogeneous Ga-rich phase, c^{II} . Assuming that the variation in concentration within the interface is gradual in comparison with the intermolecular distance, the excess free energy for the inhomogeneous region can be expanded in terms of local variables $c(\vec{r})$

and $\nabla c(\vec{r})$ ²⁸. The Gibbs free energy density cost within the interface can then be expressed in terms of a combination of a local function $g(c(\vec{r}), T)$ and a power series in $\nabla c(\vec{r})$ ^{28,34,35,36}:

$$\tilde{G} = N \int_V \left[g(c(\vec{r}), T) + \frac{1}{2} \kappa (\nabla c(\vec{r}))^2 + \dots \right] dV \quad (1)$$

where N is the number of molecules per unit volume. The function $g(c(\vec{r}), T)$ is the Gibbs free energy density that a volume would have in a homogeneous solution. The next term is the leading term in the power series expansion. The coefficient κ referred to as the influence parameter characterizes the effect of concentration gradients on the free energy. From first principles, it is related to the second moment of the Ornstein-Zernike direct correlation function and can be replaced by the pair potential weighted mean square range of intermolecular interactions of the system²⁸. Equation (1) can be considered the Landau-Ginzburg functional for this problem.

Applying (1) to the one-dimensional composition change $c(z)$ across the interface and neglecting terms in derivatives higher than the second gives for the total Gibbs free Energy \tilde{G} of the system:

$$\tilde{G} = NA_0 \int_{-\infty}^{+\infty} \left[g(c(z)) + \frac{1}{2} \kappa \left(\frac{dc(z)}{dz} \right)^2 \right] dz \quad (2)$$

The variable z represents the direction perpendicular to the interface. The symbol A_0 denotes an arbitrary surface area. The interfacial tension γ_{11} is defined as the excess energy of this inhomogeneous configuration in respect to the Gibbs free energy G of the homogeneous liquid of one of the coexisting phases. The reference system we have chosen is the homogeneous Bi-rich liquid with concentration c^I :

$$\gamma_{11} = \frac{1}{A_0} \left[\tilde{G}(c(z)) - G(c^I) \right] \quad (3)$$

Combining the gradient approximation (2) with the thermodynamic definition of the interfacial tension (3) yields:

$$\gamma_{11} = N \int_{-\infty}^{+\infty} \left[\Delta g(c(z)) + \frac{1}{2} \kappa \left(\frac{dc(z)}{dz} \right)^2 \right] dz \quad (4)$$

where the grand thermodynamic potential $\Delta g(c)$ is given by

$$\Delta g(c(z)) = g(c(z)) - g(c^I) \quad (5)$$

It follows then from (3) that the interfacial tension is a functional of the concentration profile $c(z)$ at the interface. The equilibrium surface tension is obtained by minimizing this functional leading to the following Euler-Lagrange equation:

$$\Delta g(c) = \kappa \frac{d^2 c(z)}{dz^2} \quad (6)$$

$T(^{\circ}C)$	c^I	c^{II}	$\Delta\rho_m$	$\rho/\rho_{\text{sub}}(\text{calc})$	$\rho/\rho_{\text{sub}}(\text{obs})$	q_c	d_g	d	σ_{obs}	σ_{calc}
225.0	0.39	0.91	2.30	1.24	1.25	0.0498	84.7	50	11.78	12.0
230.0	0.41	0.90	2.20	1.24	1.25	0.0499	84.9	51	14.2	13.3
235.0	0.43	0.89	2.09	1.22	1.22	0.0500	85.2	52	15.0	14.9
240.0	0.45	0.88	1.95	1.21	1.21	0.0502	85.5	53	17.5	17.25

TABLE I: Material parameters of the coexisting liquid phases as calculated from the bulk phase diagram as well as electron density profiles as obtained from our fits to R/R_F for selected temperatures T along the on-coexistence path B \rightarrow E. The atomic fraction of Ga in the coexisting Ga-rich, Bi-rich liquid phase are c^I , c^I resp. The symbols $\rho/\rho_{\text{sub}}(\text{calc})$, $\rho/\rho_{\text{sub}}(\text{obs})$ denote the calculated, observed electron density ratios resp.

This differential equation along with the boundary conditions that the concentration has to vary from c^I on the one side of the interface to c^{II} on the other side determines $c(z)$ unambiguously. In fact, the simplicity of (6) allows its direct integration, yielding an expression for $z(c)$:

$$z(c) = z_0 + \int_{c^I}^{c^{II}} \sqrt{\frac{\kappa}{\Delta g(c)}} dc \quad (7)$$

where z_0 and c_0 represent an arbitrary chosen origin and composition. It should be noted, that from a renormalization of the integrand of equation (7), one can conclude that any characteristic length scale, such as the intrinsic width of the interfacial profile, σ_{intr} , has to scale as $\sqrt{\kappa}$.

An attractive feature of this gradient theory is that it relates the profile to κ and $g(c(\vec{r}), T)$ without regard for the theoretical basis by which $g(c(\vec{r}), T)$ is derived. In this paper we will use the extended regular solution model that will be presented in the appendix to model the homogeneous Free Energy of the binary liquid metal, particularly the one used to model its miscibility gap. The sole quantity required then in order to calculate the (1/1) interfacial profile and tension is an expression for the influence parameter κ , that precedes the square gradient³⁷. It follows that the influence parameter can be extracted from the measurement of the microscopic structure of the interface. For example, from an appropriate choice for κ , solving of (6) or (7) will yield a profile characterized by the intrinsic width σ_{intr} that can be compared with σ_{obs} .

B. Capillary Wave Excitations on the (1/1) Interface

The formalism presented so far relies on a simple mean-field picture that neglects any thermal fluctuations on the (1/1) interface. By contrast, the real experiment is sensitive to not only the mean-field diffuseness of the interface, but is also sensitive to the fact that thermal fluctuations contribute additional broadening to the fluid interface. An intuitive, semiphenomenological approach to handle the interplay of these two quantities was initiated by Buff, Lovett, and Stillinger^{38,39}. Essentially, they imagined the interface as if it were a membrane in a state of tension

characterized by the bare interfacial energy γ_{II} , as calculated in the former paragraph; it sustains a spectrum of thermally activated capillary waves modes whose average energy is determined by equipartition theorem to be $k_B T/2$. By integration over the spectrum of capillary waves, one finds the average mean square displacement of the interface, σ_{cap} , as

$$\sigma_{\text{cap}}^2 = \frac{k_B T}{4\pi\gamma_{\text{II}}(\kappa)} \ln \frac{q_{\text{min}}}{q_{\text{max}}} \quad (8)$$

Here q_{max} is the largest capillary wave vector that can be sustained by the interface. For bulk liquids this is typically of the order of $\pi/\text{molecular diameter}$; however, it does not seem realistic to describe excitations with wavelengths that are smaller than the intrinsic interfacial width as surface capillary waves^{43,44}. Thus σ_{intr} describes the intrinsic interfacial width $q_{\text{max}} = \pi/\sigma_{\text{intr}}$. The value of the quantity q_{min} is slightly more complicated since it depends on whether the resolution is high enough to detect the long wavelength limit at which an external potential $v(z)$, such as either gravity or the van der Waals interaction with the substrate, quenches the capillary wave spectrum. If the resolution is sufficiently high then $q_{\text{min}} = \pi/L_v$ where $L_v^2 = \gamma_{\text{II}}^{-1} \frac{\partial^2 v(z)}{\partial z^2}$. If it is not then the value of σ_{cap}^2 is limited by the resolution limited average length scale L_{res} over which the observed fluctuations can be resolved. In this case $q_{\text{min}} = \Delta q_{\text{res}} = \pi/L_{\text{res}}$ where Δq_{res} is the projection of the detector resolution on the plane of the interface. In our case q_{res} is significantly larger than q_v therefore, $q_{\text{min}} = q_{\text{res}} = 0.04\text{\AA}^{-1}$.

Using the fact that capillary waves obey a gaussian statistics which manifests itself as an erf-function type profile for the average interfacial roughness⁴⁵ together with the observation that the intrinsic profiles $c(z)$ are also well described by erf-function profiles, the two contributions to the interfacial width can be added in gaussian quadrature⁴⁵. Thus we write the total observed interfacial width, σ_{calc} , as

$$\sigma_{\text{calc}}^2 = \sigma_{\text{intr}}(\kappa)^2 + \sigma_{\text{cap}}(\gamma_{\text{II}}(\kappa))^2 \quad (9)$$

Comparison of (8) and (6) reveals that both, σ_{intr} and σ_{cap} depend on κ . Thus, the determination of κ leads to the problem of finding the self-consistent value that yields a value for σ_{calc} that agrees with the experimentally determined roughness σ_{obs} .

C. Intrinsic Profile and (1/1) interfacial tension of Ga-Bi

We performed a self consistent calculation of κ for the observed (1/1) interface at point E, where $\sigma_{\text{obs}}(E) \approx 12\text{\AA}$. In order to do so, we solved the Euler-Lagrange Equation (6)⁷¹ which yields the intrinsic $c(z)$ profile as depicted and compared with an erf-profile in Fig. 7(a). From that we calculated the corresponding erf-diffuseness $\sigma_{\text{intr}}(E)$ and via numerical integration of (3) the corresponding interfacial tension $\gamma(E)$ as well as the resultant capillary induced roughness and the overall average diffuseness, σ_{cap} and σ_{intr} resp. After starting with a reasonable value of κ , as judged by a scaling analysis of (6), this procedure was iterated until $\sigma_{\text{calc}}(E) = \sigma_{\text{obs}}(E)$. The value we obtained was $\kappa_{\text{opt}} = 5.02 \cdot 10^{-13} \text{Nm}^3/\text{mol}$. The other quantities of interest at E are: $\sigma_{\text{cap}}(E) = 10.32\text{\AA}$, $\sigma_{\text{intr}}(E) = 6.35\text{\AA}$ and $\gamma_{\text{II}}(E) = 3.3 \text{mN/m}$.

It is interesting to observe that (6) implies $\sigma_{\text{intr}} \propto \frac{1}{\kappa}$, whereas from (8) one obtains $\sigma_{\text{cap}} \propto \sqrt{\kappa}$. Hence, the function of $\sigma_{\text{calc}}(\kappa)$ exhibits a minimum for σ_{calc} at a characteristic value, κ_{min} . It is interesting to note, that the κ_{opt} , determined from our measurements, corresponds to this peculiar value κ_{min} meaning that the system selects from all possible σ_{intr} , σ_{cap} combinations, the one with the minimum overall width for the (1/1)-interface.

Assuming a T -independent influence parameter along with the available thermochemical data sets that are available over a wide range of the phase diagram allows calculation of the T -dependent interfacial profiles and (1/1) interfacial tension from very low up to very high T , close to T_C . In Fig. 7(b) the intrinsic (1/1) interfacial profiles are plotted for selected T 's versus the reduced temperature, $t = |T - T_C|/T_C$ (Here T denotes the absolute temperature in Kelvin units). The increasing width of the interface while approaching T_C ($t \rightarrow 0$) is well-demonstrated. In Fig. 9 the t -dependent interfacial tension, $\gamma_{\text{II}}(T)$, is depicted. As expected, it vanishes as $t \rightarrow 0$.

Comparison of $\gamma_{\text{II}}(T)$ with other measurements would be a useful test of our measurements and interpretation. Unfortunately, measurements are rather difficult and we are not aware of any such measurements for Ga-Bi. Fortunately, it is still possible to estimate $\gamma_{\text{II}}(T)$ using other available experimental data sets on this alloy. For example, Predel¹⁴ noted that in the vicinity of C the (1/1)-coexistence curve of Ga-Bi can be represented by a function of the form $|\phi_c - \phi| = K(T_c - T)^\beta$ with $\beta \cong 0.33$, where ϕ is the volume fraction of Ga, Bi resp. and K a constant¹⁴. This behavior suggests that the demixing transition in Ga-Bi belongs to the same universality class as binary nonmetallic liquid mixtures, i.e. Ising lattice model with dimensionality $D=3$. Moreover, it allows for an estimation of the interfacial tension based on a scaling relation for these quantities, i.e. the hypothesis of two-scale-factor universality (TSFU)⁴⁶ should apply. Using this concept along with available T -dependent

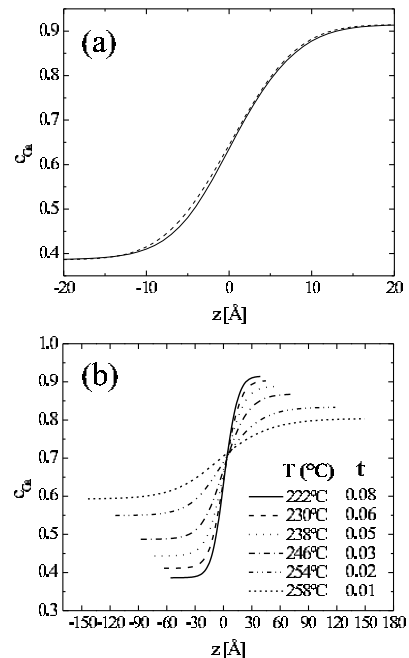


FIG. 7: (a) Calculated intrinsic profile $c(z)$ (—) for $T = T_E = 225^\circ\text{C}$, $t = 0.07$ in comparison with the erf-function profile (dashed line): $c(z) = \frac{c^{\text{I}} + c^{\text{II}}}{2} + \frac{(c^{\text{II}} - c^{\text{I}})}{2} \text{erf}\left(\frac{z}{\sqrt{2}\sigma_{\text{intr}}(E)}\right)$ with $\sigma_{\text{intr}}(E) = 6.35\text{\AA}$. (b) Calculated intrinsic concentration profiles $c(z)$ for selected temperatures T , reduced temperatures t resp. as indicated in the figure.

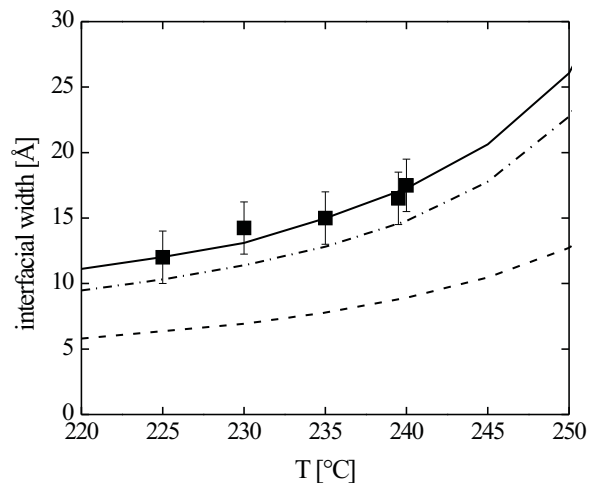


FIG. 8: Comparison of temperature dependent, measured interfacial width σ (■) with calculated interfacial widths (lines): $\sigma_{\text{calc}} = \sqrt{\sigma_{\text{intr}}^2 + \sigma_{\text{cap}}^2}$ (—), intrinsic width σ_{intr} (.-), and capillary width σ_{cap} (--).

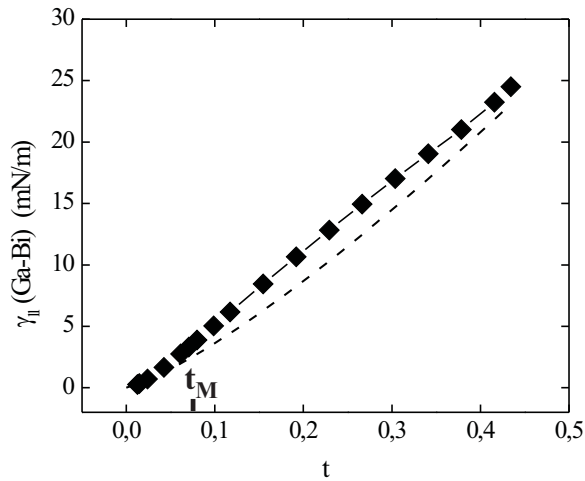


FIG. 9: Calculated (l/l) interfacial tension γ_{ll} of Ga-Bi as a function of the reduced temperature t . The dashed line represents the TSFU prediction for Ga-Bi⁴⁷. The symbol t_M indicates the monotectic temperature at $t_M(\text{Ga-Bi})=0.08$.

measurements of the specific heat, Kreuser and Woermann extracted an expression for the T -dependent interfacial tension in Ga-Bi⁴⁷, $\gamma_{ts} = \gamma_{ts0} t^\mu$, where μ is a critical exponent with universal character for a bulk demixing transition, $\mu \cong 1.26$ and $\gamma_{ts0} = 66 \pm 15 \text{mN/m}$. The corresponding t -dependent γ_{ts} (–) is plotted in Fig. 9. A good agreement with the t -dependence of γ_{ll} calculated by our square gradient theory is found, e.g. at $t_E = 0.07, T_E = 225^\circ\text{C}$: $\gamma(E) = 3.31 \text{mN/m}$, $\gamma_{ts}(E) = 5.7 \text{mN/m}$ ⁷²

D. (l/l) interfacial tension of Ga-Pb

Aside from the Ga-Bi system the only other metallic system for which detailed temperature dependent measurements⁴⁸ and estimations⁴⁹ of the (l/l) interface are reported, is Ga-Pb. Given the close relationship between Ga-Bi and Ga-Pb (similar constituents, identical phase diagram topology with consolute point C and monotectic point M), we felt encouraged to also apply our gradient theory to this binary system. Moreover, we assumed that the influence parameter, κ , as determined by the measurements on Ga-Bi, also provides a reasonable value for this metallic system. Available thermochemical data sets for the miscibility gap of Ga-Pb⁵⁰ allowed us to calculate the t -dependent (l/l) interfacial tension. As can be seen in fig. 10, where our calculated values for γ_{ll} are shown in comparison with the experimental values, an excellent agreement is found.

Overall, our results suggest that our model of an intrinsic, mean-field interface broadened by capillary waves describes the (l/l) interface reasonably well. One must,

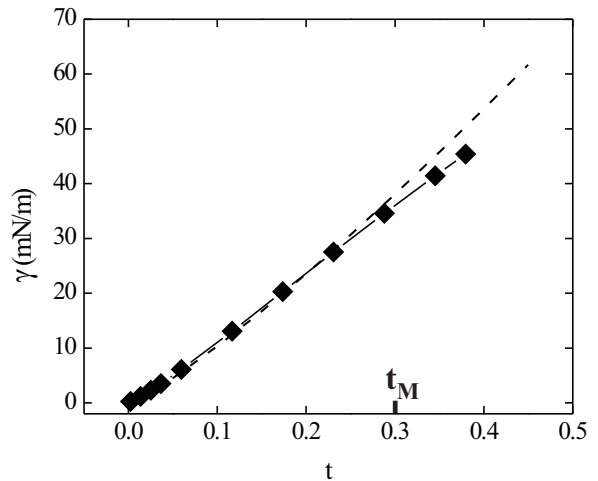


FIG. 10: Calculated (l/l) interfacial tension γ_{ll} of Ga-Pb as a function of the reduced temperature t . The solid points are our calculated values. The dashed line represents a fit to the measurements by Merkwitz et. al.⁴⁸. The symbol t_M indicates the monotectic temperature at $t_M(\text{Ga-Pb})=0.3$.

however, bear in mind the approximation implicit in the presented analysis. For instance, we have assumed that the free surface of the liquid alloy behaves like a rigid wall, whereas it will have its own spectrum of capillary waves that could be coupled to the waves at the interface. However, since the interfacial tension of the free surface is about two orders of magnitude larger than the (l/l) interfacial energy in this metallic system, we believe that the rigid wall assumption is a reasonable starting point. Furthermore, the calculation presented above has the shortcoming of a T -independent influence parameter κ . It should be mentioned, though, that theory predicts a divergence of κ close to T_C for real fluids, $\kappa \approx (T - T_C)^{-0.02}$ for $T \rightarrow T_C$. In fact, it can even be shown that this divergence is necessary to obtain the correct scaling behavior of $\gamma_{ll}(T)$ near C ^{51,52,53}.

V. WETTING PHENOMENOLOGY AT THE FREE SURFACE

1. Effects of Fluctuations on Short-Range Wetting

Our analysis in section 1 of the complete wetting transition at B was based on a mean-field (MF) model for a SRW transition. Such a model accurately predicts the critical behavior (i.e. the critical exponents) of systems close to a phase transition, provided fluctuations can be neglected. For SRW transitions, however, it can be shown that the upper critical dimensionality $D_u = 3$ ⁵⁴. The value D_u is the dimension beyond which MF theory can be applied successfully. If the dimension is smaller

than D_u fluctuations are important and one has to resort to renormalization group (RG) methods to describe the critical behavior of a phase transition. Because its upper critical dimensionality is exactly equal to 3, the SRW transition has received a great deal of theoretical attention, since it allows one to explore the regime where the MF behavior breaks down due to fluctuations, and the RG approach becomes applicable. This breakdown depends on the so-called fluctuation parameter, $\omega = k_B \cdot T / (4\pi\gamma_{\text{ll}}\xi_b^2)$ (where ξ_b is the bulk correlation length, and γ_{ll} is the (1/1) interfacial tension) which measures the magnitude of the dominant thermal fluctuations, the thermally induced capillary waves at the fluid, unbinding interface, in our case at the (1/1) interface of the coexisting Bi- and Ga-rich liquids.

For a complete wetting transition RG analysis of the divergence of the wetting film thickness yields a changed prefactor of the logarithmic divergence, $d_{\text{RG}} \sim \xi_{\text{RG}} (1 + \omega/2) \ln(1/\Delta\mu)^{5,55,56}$. An estimation of ω using the bulk correlation length, ξ_b , estimated from the aforementioned TSFU prediction, yields for the wetting transitions at M, $\omega_{\text{M}} = 0.3 \pm 0.2$ and for the observed wetting complete wetting transition at B, $\omega_{\text{B}} = 0.4 \pm 0.2$. Thus, the prefactors of the logarithmic increase of the wetting film with $\Delta\mu$ is changed by only $\approx 10\%$, 20% resp. in comparison with the mean-field prediction. This is well within our experimental error of about 30% for the determination of ξ . (The large error bar on ξ is due to its extraction from a slab thickness analysis whereas the measured wetting films have significant inhomogeneous structures). A clear distinction between RG and MF behavior cannot be drawn in our case.

A *critical* wetting transition characterized by the wetting film formation on-(1/1/v)-coexistence, while changing T , with a similar value of ω should show more pronounced deviations from MF behavior. Thus, we shall estimate the characteristic temperature T_{W} of that transition in the following.

2. The Critical Wetting Transition in Ga-Bi

It follows from our measurements that the critical wetting transition has to be hidden in the metastable range of the (1/1/v) coexistence line somewhere below T_{M} . An estimation of T_{W} is possible by a consideration of the Free energy at the surface for the wet (Bi-rich wetting at surface) and non-wet (Ga-rich phase at the surface) situation. In order to do so, we introduce the spreading energy, $\Theta(T)$. It estimates the preference of the Bi-rich phase in respect to the Ga-rich phase at the free surface at any temperature and is given by the following energetic contributions. In the wet-situation, the energy is given by the sum of the free surface tension of the Bi-rich phase and the tension of the (1/1) interface between the Bi-rich phase and the Ga-rich subphase. The non-wet situation is characterized by the surface energy of the bare Ga-rich liquid phase, $\gamma(\text{Ga} - \text{rich})_{\text{lv}}$. We define

$\Theta(T)$ therefore in the following way:

$$\begin{aligned} \Theta(T) &= \gamma(\text{Ga} - \text{rich})_{\text{lv}}(T) - \\ &\quad (\gamma(\text{Bi} - \text{rich})_{\text{lv}}(T) + \gamma_{\text{ll}}(T)) \\ &= (\gamma(\text{Ga} - \text{rich})_{\text{lv}}(T) - \gamma(\text{Bi} - \text{rich})_{\text{lv}}(T)) \\ &\quad - \gamma_{\text{ll}}(T) \\ &= \Gamma(T) - \gamma_{\text{ll}}(T) \end{aligned} \quad (10)$$

In equation (10) the quantity $\Gamma(T)$ denotes the difference in the bare liquid-vapor surface tensions of the coexisting phases.

From the definition of $\Theta(T)$ it follows that establishment of the wetting film is energetically preferred if $\Theta > 0$ (wet-situation), whereas for $\Theta < 0$ it is unfavorable (non-wet situation). The condition $\Theta(T) = 0$ marks, therefore, the transition temperature T_{W} , where the system switches on-coexistence from a non-wet to a wet-situation or vice versa.

In order to estimate $\Theta(T)$, in addition to $\gamma_{\text{ll}}(T)$, as extracted in the previous section we need measurements or estimations of $\gamma(\text{Ga} - \text{rich})_{\text{lv}}(T)$ and $\gamma(\text{Bi} - \text{rich})_{\text{lv}}(T)$. Measurements of these quantities are reported in the literature^{57,58,59}, the one by Ayyad and Freyland that employed the noninvasive method of capillary wave spectroscopy is the most recent one. From these measurements, we get a conservative T -independent estimate for Γ of the order of 100mN/m. Our calculation of $\gamma_{\text{ll}}(T)$, particularly its extrapolation towards very low temperature $t \rightarrow 1$ which yields $\gamma_{\text{ll}}(0\text{K}) = 75\text{mN/m}$, indicates that it is always significant smaller than Γ . Our analysis suggests, therefore, that $\Theta(T) > 0$ for all T meaning that *no* critical wetting transition occurs on the metastable extension of the (1/1/v) coexistence line.

This remarkable conclusion is, on the one hand, in contrast to the findings for the few examples of binary metallic wetting systems studied so far: In Ga-Pb and Ga-Tl, Wynblatt and Chatain et al. estimated a value for T_{W} significantly below the corresponding monotectic temperatures T_{M} , but still at final values of the order of $0.3 \cdot T_{\text{C}}(K)$, $0.2 \cdot T_{\text{C}}(K)$ for Ga-Pb, Ga-Tl resp. ($T_{\text{C}}(K)$ denotes the critical temperature of bulk demixing on the Kelvin temperature scale.) On the other hand, it reflects the general finding that in binary metallic systems with short-range interactions the critical wetting transition occurs at significantly lower temperatures than this is the case in organic liquid systems, where T_{W} is found to lie above $0.5 \cdot T_{\text{C}}(K)$. This tendency seems to be driven to its extreme in the case of Ga-Bi: $T_{\text{W}} = 0 \cdot T_{\text{C}}(K) = 0\text{K}$.

A semiquantitative argument for the absence of a critical wetting transition in Ga-Bi as compared to the two other metallic systems investigated so far might relate to the fact that in comparison with the others the liquid/liquid coexistence region for GaBi system is significantly shifted towards the Ga-rich, high surface tension phase and, in addition the miscibility gap is much narrower. As a result the change in concentration across the 1/1 interface is smaller for the GaBi system than for the

others. In view of the fact that one can express

$$\gamma_{ll} = \kappa \int dz \frac{dc(z)}{dz}^2 \approx \sqrt{\kappa} (\Delta c)^2 \quad (11)$$

this suggests that γ_{ll} could be expected to be smaller for GaBi than for the others. If this effect is important, and if it is not compensated by an accompanying reduction in the value of Γ , then it is possible that $\Theta(T) = \Gamma - \gamma_{ll} > 0$ for all temperatures, thereby precluding a wetting transition.

3. Tetra Point Wetting \Leftrightarrow Surface Freezing

Finally, we would like to comment on the fact that the observed wetting by the Bi rich liquid at the GaBi monotectic point is not necessarily the only phenomena that can occur. In principle one expects at this tetra point a similar or even more diverse wetting phenomenology as has been predicted⁶⁰ and found⁶¹ in the proximity of a triple point for one component systems. For example, another possibility is that the free surface could be wet by solid Bi. In the bulk both solid Bi and the Bi rich liquid are stable for $T > T_M$; however, for $T < T_M$ the free energy of the Bi rich liquid is larger than that of solid Bi. Consequently, if the solid Bi surface phase had a favorable spreading energy it would certainly wet the free surface for $T < T_M$. In fact, on the basis of optical and surface energy measurements Turchanin et al.^{62,63} proposed a surface phase diagram for which a surface frozen" phase of solid Bi forms at the free surface of the GaBi liquid for temperatures below T_M . Unfortunately, we have a problem with this. The first may be purely semantic, but the idea of a "surface frozen phase" originates in the experiments by Earnshaw et al. and Deutsch, Gang, Ocko et al^{64,65} on the appearance of solid surface phases at temperatures above that of bulk freezing for alkanes and related compounds. For the GaBi system the crystalline phase of bulk Bi is stable at temperatures well above those of at which Turchanin et al made their observations. We believe that if their observations do correspond to thermal equilibrium phenomena, the effect would be more appropriately described as wetting of the free surface by solid Bi. Unfortunately, the second problem we have is that we do not believe that surface wetting by solid Bi is favored by the spreading energy. If wetting by solid Bi were favored, as implied by Turchanin et al, then the wetting layers of Bi rich liquid that are the subject of this paper would have to be metastable, existing only because of a kinetic barrier to the nucleation of the solid wetting film. In fact we have regularly observed that on cooling below T_M the original fluid, smooth, highly reflecting surfaces became both rough and rigid. The effect is exacerbated by the presence of temperature gradients and by rapid cooling. We interpreted this as the formation of bulk solid Bi, rather than wetting, since we never saw any direct evidence for the formation of films, rather than bulk Bi. We argued that if there not enough time

for the excess Bi in the bulk liquid phase below the surface to diffuse, and precipitate as bulk solid Bi at the bottom of the liquid pan, the bulk liquid would simply undergo bulk spinodal phase separation. This is consistent with our observations. Unfortunately it is very difficult to absolutely prove that our films are stable and this issue can't be resolved from the existing evidence. Nevertheless we find it difficult to understand why solid Bi would wet the surface for $T < T_M$ and not wet the surface as T approaches T_M from above.

VI. SUMMARY

In this paper we reported x-ray reflectivity measurements of the temperature dependence of wetting phenomena that occur at the free surface of the binary metallic alloy Ga-Bi when the bulk demixes into two liquid phases, i.e. a Bi-rich and a Ga-rich liquid phase. We characterized the temperature dependence of the thickness and interfacial profile, with Ångström resolution, of the Bi-rich wetting films that form at the free surface of the liquid on approaching the (1/1/v) coexistence triple line, i.e. along a path of complete wetting. The results, which are characterized by large concentration gradients, agree with density functional calculations for such transitions at hard walls. On the basis of this it was possible to determine the short-range surface potential that favors the Bi-rich phase at the free surface and hence is governing the wetting phenomenology. The short-range *complete wetting* transition turns out to be only marginally affected by thermal fluctuations. According to renormalization group analysis the *critical wetting* transition should be more sensitive to critical fluctuations; however, according to our analysis the wetting layer of Bi rich liquid should be present for all temperatures. This is in contrast to the results for the other binary liquid metal systems for which the wetting transitions exists but since the metastable 1/1/v line it falls below the liquidus line it is hidden.

The largest thickness of the gravitationally limited Bi rich wetting layers that formed at the free surface at (1/1/v)-coexistence were typically of the order of $\approx 50\text{Å}$. As a result of the fortuitous balance between the surface potential that favors the Bi-rich Phase and the gravitational potential which favors the lighter Ga-rich phase the interface dividing the two coexisting phases is sufficiently close to the free surface that x-ray reflectivity was sensitive to its microscopic structure. We interpreted these measurements in terms a Landau type of square gradient phenomenological theory from which it was possible to extract the sole free parameter of that model, i.e. the influence parameter κ . To the best of our knowledge this is the first time that such a parameter has been directly determined from measurement. Furthermore, it was possible to make a distinction between the intrinsic width of the interface and the additional contributions to the width from thermal capillary wave features fluctuations.

On making use of available bulk thermodynamic data, along with the extracted influence parameter, we were able to calculate the experimentally difficult to get (1/1) interfacial tension for a wide temperature range. As a test of our methods we performed the same calculation of the (1/1) interfacial tension for Ga-Pb with its analogous miscibility. We assumed that the influence parameter, κ , as determined from our measurements on the (1/1) interfacial structure in Ga-Bi, was also applicable to Ga-Pb and, using the thermochemical data sets available for Ga-Pb, we obtained good agreement between our calculated values and macroscopic measurements of the (1/1) interfacial tension. This suggests that the value of the influence parameter extracted in this study might provide a reasonable value for the larger class binary metallic alloys. If this proves to be true, then the value determined here can be used, along with the surface potential, to predict wetting properties of this larger class of systems.

Acknowledgments

We thank Prof. S. Dietrich and Prof. B. I. Halperin for helpful discussions. This work is supported by U.S. DOE Grant No. DE-FG02-88-ER45379, National Science Foundation Grant DMR-0124936, and the U.S.-Israel Binational Science Foundation, Jerusalem. BNL is supported by U.S. DOE Contract No. DE-AC02-98CH10886. Patrick Huber acknowledges support from the Deutsche Forschungsgemeinschaft.

APPENDIX: BULK THERMODYNAMICS

Here⁷³, we focus on the part of the phase diagram dominated by the miscibility gap and the monotectic point M. In a liquid-liquid (l/l) equilibrium of binary systems, consisting of two components (Ga and Bi resp.), at atmospheric pressure p , temperature T , the compositions c_I , c_{II} of two coexisting bulk phases (I and II) are given by the thermodynamic conditions:

$$\mu_{\text{Ga}}^I(T) = \mu_{\text{Ga}}^{II}(T) \quad \mu_{\text{Bi}}^I(T) = \mu_{\text{Bi}}^{II}(T) \quad (\text{A.1})$$

where μ is the chemical potential. The experimental conditions of the experiments that we are going to present are constant temperature, pressure and a fixed number of moles of each component, therefore we have to resort to the Gibbs free energy G in order to describe the thermodynamic equilibrium:

$$G = U - TS + PV \quad (\text{A.2})$$

$$G = n g = n_{\text{Ga}} \mu_{\text{Ga}} + n_{\text{Bi}} \mu_{\text{Bi}} \quad (\text{A.3})$$

Since the total number of particles in mol $n = n_{\text{Ga}} + n_{\text{Bi}}$ is constant and only two components have to be considered, the system can be described with a molar Gibbs Free Energy $g(c, T)$ that depends on only on the molar fraction

of one component:

$$G = n (c \mu_{\text{Ga}} + (1 - c) \mu_{\text{Bi}}) \quad (\text{A.4})$$

$$\Rightarrow g(c, T) = c \mu_{\text{Ga}} + (1 - c) \mu_{\text{Bi}} \quad (\text{A.5})$$

With this notation the phase equilibrium conditions (equation (A.1)) transform into the following two equations:

$$\left. \frac{\partial g}{\partial c} \right|_{c^I} = \left. \frac{\partial g}{\partial c} \right|_{c^{II}} \quad (\text{A.6})$$

$$\left. \frac{\partial g}{\partial c} \right|_{c^I} = \frac{g(c^I) - g(c^{II})}{c^I - c^{II}} \quad (\text{A.7})$$

Having a model for the free energy of a binary system, it is possible, then, to calculate c_I and c_{II} of the coexisting phases by solving of equation (A.7). The standard approach to describe a miscibility gap in a binary demixing system is the regular solution model for the Gibbs free energy⁶⁶. The resulting miscibility gap has a symmetric shape and is centered around the consolute point $c_{\text{crit}} = 0.5$ in the (c, T) -plane, quite in contrast to the miscibility gap of Ga-Bi with its asymmetric shape, centered around $c_{\text{crit}} = 0.7$ in the (c, T) -plane. Therefore, it is necessary to resort to an *extended* regular solution model. Relying on data sets for Ga-Bi from the Calphad initiative¹⁵, we use such a model based on Redlich-Kister polynomials $L_\nu(T)$ ^{67,68} and express $g(c, T)$ in the following way:

$$g(c, T) = c \cdot g_0(\text{Ga})(c, T) + (1 - c) \cdot g_0(\text{Bi}) \\ + R \cdot T [c \ln(c) + (1 - c) \ln(1 - c)] \\ + \Delta g_{\text{mix}}(c, T) \quad (\text{A.8})$$

$$\Delta g_{\text{mix}}(c, T) = c(c - 1) \sum_{\nu=1}^5 L_\nu(T) (1 - 2c)^\nu$$

The first two terms correspond to the Gibbs energy of a mechanical mixture of the constituents; the second term corresponds to the entropy of mixing for an ideal solution, and the third term, Δg_{xs} is the so-called excess term. Here, it is represented by an extension of the usual regular solution expression, i.e. a sum of Redlich-Kister polynomials, $L_\nu(T)$, as listed in Table II.

By solving the nonlinear equations (A.7) applied on $g(c, T)$ for the temperature range $T_M < T < 262^\circ\text{C}$ we could calculate the binodal coexistence line as plotted in Fig. 1. The agreement of the calculated phase boundaries with Predel's measured phase boundaries is excellent. Particularly, the measured consolute point C ($T_C = 262^\circ\text{C}$, $c_{\text{crit}} = 0.7$) is nicely reproduced by the calculated critical values $T_C = 262.8^\circ\text{C}$ and $c = 0.701$. Furthermore, the knowledge of $g(c, T)$ allows us to extrapolate the binodal lines below T_M into the region of metastable (l/l) coexistence, and, hence, to get information on the energetics of the metastable Ga-rich, Bi-rich phase resp. Similar to the procedure presented above, we

ν	Redlich-Kister polynomial $L_\nu(T)$
0	80000-3389+T
1	-4868-2.4342·T
2	-10375-14.127·T
3	-4339.3
4	2653-9.41·T
5	-2364

TABLE II: Redlich-Kister polynomials used to model the (l/l) miscibility gap of Ga-Bi^{15,67}.

also calculated the phase boundaries below T_M . Here, we used data sets for the Gibbs free energy of pure solid Bi, which coexists for $T < T_M$ with a Ga-rich liquid.

- * Electronic address: p.huber@mx.uni-saarland.de; present address: Fakultät für Physik und Elektrotechnik, Universität des Saarlandes, 66041 Saarbrücken, Germany
- ¹ J. W. Cahn, J. Chem. Phys. **66**, 3667 (1977).
 - ² C. Ebner and W. F. Saam, Phys. Rev. Lett. **38**, 1486 (1977).
 - ³ P. G. de Gennes, Rev. Mod. Phys. **57**, 827(1985).
 - ⁴ D. E. Sullivan and M. M. T. da Gama, *Fluid Interfacial Phenomena*, edited by C. A. Croxton (Wiley, New York), (1986).
 - ⁵ S. Dietrich, in C. Domb and J. L. Lebowitz (Eds.), *Phase Trans. and Crit. Phen.*, Vol. 12, Acad. Press, NY, 1988.
 - ⁶ B. M. Law, *Progress in Surface Science* **66**, 159 (2001).
 - ⁷ D. Bonn, D. Ross, *Rep. Prog. Phys.* **64**, 1085 (2001).
 - ⁸ A. Plech, U. Klemradt, M. Huber, J. Peisl, *Europhys. Lett.* **49**, 583(2000).
 - ⁹ H. Tostmann, E. DiMasi, O. G. Shpyrko, P. S. Pershan, B. M. Ocko, M. Deutsch, *Phys. Rev. Lett.* **84**, 4385 (2000).
 - ¹⁰ M. L. Schlossman, *Curr. Opinion Coll.&Interf. Sc.* **7**, 235 (2002).
 - ¹¹ D. Chatain and P. Wynblatt, *Surface Science* **345**, 85 (1996).
 - ¹² H. Shim, P. Wynblatt, D. Chatain, *Surface Science* **476**, L273 (2001).
 - ¹³ D. Natland, P. D. Poh, S. C. Müller, W. Freyland, *J. Phys. C* **7**, L457 (1995).
 - ¹⁴ P. Predel, *Z. f. Phys. Chemie Neue Folge* **24**, 206 (1960).
 - ¹⁵ The calculations of the phase boundaries rely on data sets for Ga-Bi from the CalPhaD initiative (Larry Kaufman (MIT)), which have been refined in order to more accurately reproduce Predel's phase diagram¹⁴.
 - ¹⁶ J. H. Perepezko, C. Galang, K. P. Cooper in G. E. Rindone (ed.), *Materials Processing in the Reduced Gravity Environment of Space*, Elsevier (Amsterdam) p 491 (1982).
 - ¹⁷ N. Lei, Z. Q. Huang, and S. A. Rice, *J. Chem. Phys.* **104**, 4802 (1996).
 - ¹⁸ S. Dietrich and M. Schick, *Surface Science* **382**, 178 (1997).
 - ¹⁹ P. Huber, O. G. Shpyrko, P. S. Pershan, B. M. Ocko, E. DiMasi, M. Deutsch, *Phys. Rev. Lett.* **89**, 035502 (2002).
 - ²⁰ M. J. Regan, P. S. Pershan, O. M. Magnussen, B. M. Ocko, M. Deutsch, L. E. Berman, *Phys. Rev. B* **55**, 15874 (1997).
 - ²¹ P. S. Pershan and J. Als-Nielsen, *Phys. Rev. Lett.* **52**, 759 (1984).
 - ²² P. S. Pershan, *Phys. Rev. E* **50**, 2369 (1994).
 - ²³ M. Tolan, *X-Ray Scattering from Soft-Matter Thin Films*, Springer Tracts in Modern Physics **148** (1998).
 - ²⁴ L. G. Parratt, *Phys. Rev.* **95** 358 (1954).
 - ²⁵ R. Lipowsky, D. A. Huse, *Phys. Rev. Lett.* **57**, 353 (1986).
 - ²⁶ X. L. Wu, M. Schlossman, C. Franck, *Phys. Rev. B* **33**, 402 (1986).
 - ²⁷ D. Fenistein, D. Bonn, S. Rafai, G. H. Wegdam, J. Meunier, A.O. Parry, M.M.T. da Gama, *Phys. Rev. Lett.* **89**, 096101 (2002).
 - ²⁸ H. T. Davis, *Statistical Mechanics of Phases, Interfaces, and Thin Films*, Wiley-VCH, NY (1996).
 - ²⁹ F. Schmid, N. B. Wilding, *Phys. Rev. E* **63**, 1201 (2001).
 - ³⁰ A. Plech, U. Klemradt, J. Peisl, *J.Phys. C* **13**, 5563 (2001).
 - ³¹ D. Fenistein, D. Bonn, S. Rafai, G. H. Wegdam, J. Meunier, A. O. Parry, M. M. T. da Gama, *Phys. Rev. Lett.* **89**, 096101 (2002).
 - ³² N. W. Ashcroft, *Phil. Trans. R. Soc. Lond. A* **334**, 407 (1991).
 - ³³ B. Pluis, T. N. Taylor, D. Frenkel, J.F. van der Veen, *Phys. Rev. B* **40** 1353 (1989).
 - ³⁴ J. D. van der Waals, *Z. Phys. Chem.* **13** (1894).
 - ³⁵ J. W. Cahn, J. E. Hilliard, *J. Chem. Phys.* **28**, 258 (1958).
 - ³⁶ S. A. Safran, *Statistical Thermodynamics of Surfaces, Interfaces, and Membranes*, *Frontiers in Physics*, ed. David Pines, Westview Press (1994).
 - ³⁷ S. Enders, K. Quitzsch, *Langmuir* **14**, 4606 (1998).
 - ³⁸ F. P. Buff, R. A. Lovett, F. H. Stillinger, *Phys. Rev. Lett.* **15** 621 (1965).
 - ³⁹ J. S. Rowlinson, B. Widom, *Molecular Theory of Capillary*, Clarendon Press, Oxford (1982).
 - ⁴⁰ B. M. Ocko, X. Z. Wu, E. B. Sirota, S. K. Sinha, M. Deutsch, *Phys. Rev. Lett.* **72**, 242 (1994).
 - ⁴¹ R. K. Heilmann, M. Fukuto, P. S. Pershan, *Phys. Rev. B* **63**, 5405 (2001).
 - ⁴² A. Braslau, P. S. Pershan, G. Swislow, B. M. Ocko, J. Als-Nielsen, *Phys. Rev. A* **38**, 2457 (1988).
 - ⁴³ T. Wadewitz, J. Winkelmann, *Phys. Chem. Chem. Phys.* **1**, 3335 (1999).
 - ⁴⁴ R. Evans, *Mol. Phys.* **42**, 1169 (1981).
 - ⁴⁵ J. Dailant, A. Gibaud, *X-Ray and Neutron Reflectivity: Principles and Applications*, *Lecture Notes in Physics*, Springer (1999).
 - ⁴⁶ D. Stauffer, M. Wortis, M. Ferer, *Phys. Rev. Lett.* **29**, 345 (1972).
 - ⁴⁷ H. Kreuser and D. Woermann, *J. Chem. Phys.* **98**, 7655 (1993).
 - ⁴⁸ M. Merkwitz, J. Weise, K. Thriemer, W. Hoyer, *Zeitschrift für Metallkunde* **89**, 247 (1998).

- ⁴⁹ P. Wynblatt, A. Saul, D. Chatain, *Acta Metallurgica* **46**, 2337 (1998).
- ⁵⁰ I. Ansara, F. Ajersch J. Phase Equilibria **12** 73 (1991).
- ⁵¹ P. M. W. Cornelisse, C. J. Peters, J. de Arons, *J. Chem. Phys.* **106**, 9820 (1997).
- ⁵² S. Fisk, B. Widom, *J. Chem. Phys.* **50**, 3219 (1969).
- ⁵³ J. V. Sengers, J. M. J. VanLeeuwen, *Phys. Rev. A* **39**, 6346 (1989).
- ⁵⁴ M. Schick, in J. Charvolin, J. F. Joanny, J. Zinn-Justin (Eds.), *Liquids at Interfaces*, Vol. XLVIII, p. 419.
- ⁵⁵ E. Brezin, B. I. Halperin, S. Leibler, *Phys. Rev. Lett.* **50**, 1387 (1983).
- ⁵⁶ D. M. Kroll, R. Lipowsky, R. K. P. Zia, *Phys. Rev. B* **32**, 1862 (1985).
- ⁵⁷ K. B. Khokonov, S. N. Zadumkin, *Sov. Electrochem.* **10**, 865 (1974).
- ⁵⁸ A. H. Ayyad, W. Freyland, *Surf. Science* **506**, 1 (2002).
- ⁵⁹ A. H. Ayyad, I. Mechdiev, W. Freyland, *Chem. Phys. Lett.* **359**, 326 (2002).
- ⁶⁰ R. Pandit, M.E. Fisher, *Phys. Rev. Lett.* **51** 1772 (1983).
- ⁶¹ G. Zimmerli, M. H. W. Chan, *Phys. Rev. B* **45**, 9347 (1992).
- ⁶² A. Turchanin, D. Nattland, W. Freyland, *Chem. Phys. Lett.* **337**, 5 (2001).
- ⁶³ A. Turchanin, W. Freyland, D. Nattland, *Phys. Chem. Chem. Phys.* **4**, 647 (2002).
- ⁶⁴ J. C. Earnshaw, C. J. Hughes, *Phys. Rev. A* **46**, R4494 (1992).
- ⁶⁵ X. Z. Wu, R. Sikorski, S. K. Sinha, B. M. Ocko, M. Deutsch, *Phys. Rev. Lett.* **70**, 958 (1993).
- ⁶⁶ P. W. Atkins, *Physical Chemistry*, W.H. Freeman (2001).
- ⁶⁷ U. R. Kattner, *JOM-J. Minerals Metals& Mat. Soc.* **49**, 14 (1997).
- ⁶⁸ H. L. Lukas, J. Weiss, and E.-Th. Henig, *CALPHAD*, **6** 229 (1982).
- ⁶⁹ D. Maede, B. S. Haran, R. E. White, *MapleTech* **3**, 85 (1996).
- ⁷⁰ Additionally, the (s/l/v) triple line due to the coexistence of a Bi-rich liquid, a pure Bi solid, and the vapor phase - cp. the left side of the (c,T) phase diagram (Fig. 1) starts at M. Since it is not relevant for the considerations of the wetting thermodynamics at the surface, it is not shown in Fig. 2(a),(b) for the sake of simplicity.
- ⁷¹ We used the standard procedures for solving differential equations included in the *Maple 7* software package (Waterloo Maple Inc.) as well as the "*Shooting Technique for the solution of two-point boundary value problems*" as implemented for this software package by D.B. Maede⁶⁹.
- ⁷² In the strict sense, the TSFU hypothesis is only valid in a T -range, where mapping of the demixing process on a second order phase transition is justified, which is typically the case for reduced temperatures, $t < 10^{-1}$. Despite of this restriction, it often fits well experimental results⁴⁸ and obviously also our results of the gradient theory in a much wider temperature range.
- ⁷³ Note unless it is explicitly indicated otherwise, in this chapter " T " denotes the absolute temperature in Kelvin units.